

Article

Skyfall 2020: Smartphone data from a 36 km drop

Milton Garcés ^{1,2}, Daniel Bowman ³, Cleat Zeiler ⁴, Anthony Christe ², Tyler Yoshiyama ¹, Brian Williams ¹, Meritxell Colet ¹, Samuel Takazawa ¹, Sarah Popenhagen ¹, Yusuke Hatanaka ¹, Jonathan Tobin ^{1,5}, Kale McLin ⁴

¹ Infrasound Laboratory, University of Hawaii, Manoa, HI 96740, USA; milton@isla.hawaii.edu

² RedVox, Inc., Kailua-Kona, HI 96740, USA

³ Sandia National Laboratories, Albuquerque, NM 87123, USA

⁴ Nevada National Security Site, Nevada, USA

⁵ Augustus Aerospace Company

Abstract: A smartphone plummeted from a stratospheric height of 36 km (~119,000 feet), providing a complete record of its rapid descent and abrupt deceleration when it hit the ground. The smartphone was configured to collect internal sensor data at high rates. We discuss the state-of-the-art of smartphone environmental and sensing capabilities at the closing of year 2020 and present a flexible mobile sensor data model. The associated open-source application programming interface (API) and python software development kit (SDK) used in this work is transportable to any hardware platform and operating system.

Keywords: smartphones; balloons, internet of things; cyber-physical systems

1. Introduction

A smartphone was hoisted by a helium-filled mylar balloon over southern Nevada, USA, to capture high-altitude acoustic signatures from a surface chemical explosion on October 27, 2020 [1]. The smartphone was running the RedVox [2, 3] application to collect geophysical and state of health information using its on-board sensors. Additional location and barometric pressure information was provided by a HAB Bouncer Balloon Cut-Down Device [4]. The balloon reached an altitude of 36.3 km before the payload was released and fell back to Earth. The payload descent through the stratosphere and troposphere was slowed down by a parachute. Although the landing was abrupt – as expected from a non-steerable canopy - the instruments were recovered intact and have been deployed in subsequent missions.

This paper concentrates on the geophysical data recorded by the smartphone during its rapid descent until hits the ground ~30 minutes later. Signals from the explosion are explicitly excluded in this work as they are part of separate studies [1, 5].

The primary aims of this paper are to demonstrate how commercial, off-the-shelf smartphones can be viable geophysical data collection platforms and to provide algorithms and open-source code to access their digital sensor data. We describe one approach to handling these data under the RedVox Application Programming Interface (API) [6] and associated Software Development Kit (SDK) [7]. The RedVox-Pandas [8] framework builds on the Pandas [9] serialized data structures and is used to process the smartphone data. The raw data [10] and open-source code [8] used in this paper are provided, and a reader with minimal Python experience should be able to reproduce the results.

Since smartphones and their kindred cyber-physical platforms are rapidly evolving, this paper will only be a snapshot of the technology at the closing of the year 2020. To compensate for this rapid obsolescence cycle, we also report on present-generation RedVox API 1000 (API M) which was released globally in June 2021 through the Google Play and Apple App stores. Some of the merits and limitations of the API 900 deployed in 2020 are highlighted, with strategies to overcome known issues. The RedVox SDK converts now-obsolete API 900 to the current API M field specifications.

As of the time of this writing, data collection and transmission under API M has been implemented in Android, iOS, Linux, and Mac OS operating systems.

2. Materials and Methods

This paper presents data collected during the Skyfall plunge, starting at a height of ~36 km a few seconds before the initiation of descent and ending on the ground. The raw smartphone data are available at <http://redvox.io/@3f3f> [6]

Although human-readable local time is more readily accessible in daily life, our computations use Unix time (also referred to as the *epoch* time) UTC, the number of seconds since 1 January 1970 relative to the Greenwich meridian. Although our highest sample rate was only 8 kHz, present-day smartphone audio systems are able to record at 192 kHz, corresponding to a sampling interval of 5.2 microseconds. Throughout this work, the native unit of time for computations is epoch in microseconds.

2.1. Balloon platform

The flight system consisted of a 4 kg Totex [11] weather balloon carrying a 2.25 kg instrumentation package (Figure 1). The flight line consisted of a 10 m paracord tether from the balloon nozzle to a Balloon Ascent Technologies HAB Bouncer Balloon Cut-Down Device [4]. The Bouncer was geofenced to automatically terminate the flight if the balloon approached the Las Vegas metro area. The Bouncer was connected to a fishing swivel, which was tied to the top loop of a 4 ft Rocketman parachute [12]. The descent rate for the 4 ft (1.21 m) standard parachute at 5 lbs (2.3 kg) is specified at 20ft/s (6 m/s ~ 21 km/h). The fishing swivel allows the payload to rotate independently of the balloon, which tends to prevent violent spinning during ascent. A High-Altitude Science Stratotrack APRS (Automated Packet Reporting System) [13] transmitter beneath the parachute was intended to provide one minute balloon location and ambient temperature readings during flight.



Figure 1. A meteorological balloon carrying infrasound sensors in a PolarTech insulated shipping container in 2015. The parachute is visible between the box and the balloon. The Skyfall setup is very similar to the one described here.

The key elements of the payload box consisted of a PolarTech insulated shipping carton containing a SPOT Trace [14] asset tracker to report the landing location, and a Samsung Galaxy S10 [15] in a protective case taped screen-down to the bottom of the box. The dimensions of the payload box were L15" x W13" x H10" (~38.1 cm long, 33 cm wide, and 25.4 cm high); the rectangular shape of the payload enclosure may have helped stabilize the descent, as the vertical axis remained relatively stable until impact. The payload box was sealed with duct tape prior to launch, but a hole in the side allowed a venting tube to pass between the outside air and the interior of the box.

There were four independent instruments for estimating location; however, two of the four instruments only provided sparse estimates intended for recovery. The APRS and SPOT trace were primarily intended to provide redundancy for the payload recovery. Only the Bounder and the S10 smartphone had sufficiently high sample rates to reconstruct the details of the rapid descent trajectory, and both of these instruments had a barometer to provide secondary height estimates. The Bounder relies exclusively on the Global Navigation Satellite System (GNSS) for position, whereas the S10 uses both GNSS and cellular location when available. Only the RedVox S10 used a cellular network to transmit data in real time when possible.

The balloon was inflated in a hangar from Desert Rock Airport, then launched at 12:16 UTC, October 27, 2020 into a brisk wind blowing to the south/southwest. The APRS tracker provided the balloon's location every minute until it became too cold during the early dawn ascent. It resumed reporting positions once the sun had risen above the horizon and the unit had risen high enough in the stratosphere for ambient temperatures to come back into range.

The balloon burst at 13:47:50 UTC at an altitude of 36,296 m, landing at 14:13:25 UTC at an elevation of 1,038 m. Landing was first indicated by the RedVox phone, which reported that it was no longer moving and that the ambient temperature was rising as the payload box warmed up after landfall. The SPOT Trace then confirmed the landing site. The payload was recovered at 1700 UTC on the same day. The payload box was upside down, and large amounts of balloon material was tangled on the flight line and the parachute (Figure 2). This suggests that the parachute may not have deployed properly and that the payload may have descended faster than planned. Although the box was externally scraped after the landing, the S10 was undamaged and has been redeployed in other missions.



Figure 2. Landing site, with payload box flipped upside down on the lower right and the parachute (blue and red) tangled with balloon shreds in the upper left.

2.2. *Bounder*

We use the Balloon Ascent Technologies HAB Bounder™ Balloon Cut-Down Device [4] as a primary reference for the balloon trajectory. Unlike smartphones, the Bounder is designed for high-altitude balloons (HAB) so its barometer specifications are better matched to the 36 km balloon height. Furthermore, the Bounder provides a continuous record, whereas the smartphone location has a gap at the higher altitudes.

The Bounder exports balloon GNSS location and barometric pressure data collected at a rate of ~ 1 Hz to a text file. Per the documentation sheet, the pressure rating on the Bounder barometer is 8 to 1200 hPa (0.8 – 120 kPa). The Bounder trajectory fields and observations for the event of interest are presented in Tables 1 and 2 and shown in Figure 3; this paper concentrates on the rapid descent after the peak height shown to the right of the red arrow in Figure 3. The Bounder's peak recorded elevation at 13:47:50 GMT was 36,296 m above the WGS84 geoid, and the balloon was still ascending before the payload release.

Table 1. Boulder Event Information

Description	Value
Start Date Time	2020-10-27 13:45:00
Start Epoch s	1603806300
Start Latitude degrees	36.07616
Start Longitude degrees	-115.62339
Start Altitude m (WGS-84)	35538
Stop Date Time	2020-10-27 14:16:00
Start Epoch s	1603808160
Stop Latitude degrees	35.83728
Stop Longitude degrees	-115.57234

Table 2. Boulder Location Sensor

Description	Field	Units
Pres	Atmospheric pressure	hPa = mbar
Lon /Lat	GNSS longitude and latitude	degree decimal
Alt	GNSS altitude above ellipsoid	meters
Date	GNSS date	YYYYMMDD
Time	GNSS time	HH:MM:SS
Sample Interval	1.004, Derived from Time	seconds
Interval St Dev	0.061, Derived from Time	seconds



Figure 3. Balloon trajectory for complete event. The Skyfall data concentrates on the rapid descent.

2.3. Smartphone

All modern-day commercial-off-the-shelf (COTS) smartphones come loaded with a suite of advanced small weight, power, and cost (SWAP-C) sensors. From the beginning, all mobile phones contain a microphone (mic) for voice communication. Starting with flip phones and continuing with smartphones, cameras shortly followed, with accelerometers, gyroscopes, barometers, and other more esoteric sensor modalities. All operating systems (OSs) have an Application Programming Interface (API) to access data from internal sensors. An API is a formal definition of inputs and outputs for a given computational system. The API describes what fields or methods are available, the data and types of data that can be accepted, and the data and types of data that can be returned. An API provides a contract and documentation to a developer for how to interact with a given system. This paper concentrates on the RedVox APIs [6].

RedVox APIs are tailored for collecting a wide range of heterogeneous sensor data from distributed stations running on diverse OSs. The current version, at the time of this writing, is API 1000 (API M), although API (version number 900) was utilized for this event. Google's Protocol Buffers were used when designing API 900 and API M, allowing them to be accessed from multiple programming languages. The API is designed to store both device-specific metadata as well as diverse user-specified sensor data. Metadata includes station identification information as well as a summary of the station's hardware and configuration.

The API accepts data from a wide range of sensor hardware. This includes sensors with stable, (mostly) evenly spaced sampling rates such as audio, sensors with unevenly spaced sampling rates, single channel sensors, and multi-channel sensors. The API includes enhanced metadata for the storage of location information and for the storage of timing and timing correction information.

Data are quantized into individual files called packets. The duration of a packet is determined by the requested number of audio samples stored in the packet for a given sampling rate. Packets are compressed for both transport and storage using the LZ4 compression algorithm. The packets are always stored on the device, and are also streamed to the RedVox server in the Amazon Web Services cloud if either cellular or wifi communications are available. Data packets collected during the Skyfall were transmitted over the cellular network in flight and after landing.

API M expands on the types of metadata stored with each packet with an emphasis on storing SWAP-C metrics. API M also provisions for storing real-time, edge-computed event results derived on stations at runtime.

Associated with the API is a Software Developer Kit (SDK) [7] which facilitates access to the API fields. The purpose of the SDK is to provide a wide range of tools to acquire, process, and analyze the data. The SDK functions on a variety of configurations of hardware and software, and should produce the consistent result when run across each of the configurations.

The components of the SDK critical to Skyfall are the Station and DataWindow objects. A Station object represents a single device, which we refer to as a *Station*. Each Station is capable of holding a variety of data from various sensors (e.g. audio, barometer, location, accelerometer, gyroscope and magnetometer). A DataWindow object is a grouping of Station objects with a defined start and end datetime, and is created by loading and processing raw API M or API 900. DataWindow is intended for export to more traditional geophysical data formats such as miniseed or SAC, or converted to other data structures for analysis by data scientists.

A Samsung Galaxy S10 station was deployed for the Skyfall collection, and the high-level specifications returned by the Android OS to the RedVox SDK are provided in Table 3.

Table 3. Smartphone Station Specifications

Description	Field	Value
Station ID	station.id	1637610021
Make	station.metadata.make	samsung
Model	station.metadata.model	SM-G973U1
OS	station.metadata.os	ANDROID
OS Version	station.metadata.os_version	10
App Version	station.metadata.app_version	2.6.20
SDK Version	station.metadata.os_version	3.0.0rc37

As of the time of this writing, the Android RedVox application is supported by >10,000 different Android smartphone and tablet models, not including Chrome notebooks and other devices running Android virtual machines.

For the purposes of the Skyfall event, there are three defining timescales of importance: the start of the clock (station start date), the start of the event, and the end of the event. Although the precision of these time scales are microseconds, only the corresponding epoch times in seconds are shown on Table 4. The station clock resets every time the app is stopped and started, and the station recording parameters can only be changed if the app recording is stopped. Therefore, it is possible to identify a station and its data collection settings during a recording session by its Station ID (Table 3) and its Station Start Date (Table 4).

Table 4. Station and Event Date

Description	Field	Epoch s	Human UTC
Station Start Date ¹	station.start_timestamp	1603719281	2020-10-26 13:34:41
Event Start Date	station.first_data_timestamp	1603806314	2020-10-27 13:45:14
Event End Date	station.first_data_timestamp	1603808114	2020-10-27 14:15:14

¹ Not available before v.2.6.3

2.3.1. Microphone

Since sound quality is a key competitive feature between makes and models, Original Equipment Manufacturers (OEMs) are protective of their microphone specifications and configurations. It is neither possible nor practical to characterize the response of the >10,000 different models of smartphones in the market, although some traditional methods have been pursued [16, 17]. We work with the raw digital, uncalibrated output and concentrate on the signal to noise ratio (SNR) of the observed signal. The nominal and observed sample rate of the primary internal front-facing smartphone microphone are presented in Table 5.

Table 5. Audio Sensor

Description	Field	Value
Sensor Name	station.audio_sensor().name	I/INTERNAL MIC
Nominal Rate Hz	station.audio_sample_rate_nominal_hz	8000
Sample Rate Hz	station.audio_sensor().sample_rate_hz	8000.043426
Sample Interval s	station.audio_sensor().sample_interval_s	0.000124999
Interval Standard Deviation s	station.audio_sensor().sample_interval_std_s	5.20E-08

2.3.2. Barometer

The specifications for the station barometer obtained through the Android framework under RedVox API900 are listed in Table 6.

Table 6. Barometer Sensor

Description	Field	Value
Sensor Name	station.barometer_sensor().name	LPS22HH Barometer
Sample Rate Hz	station.barometer_sensor().sample_rate_hz	24.40309971
Sample Interval s	station.barometer_sensor().sample_interval_s	0.040978401
Interval Dev s	station.barometer_sensor().sample_interval_std_s	0.006281194

The pressure range of STMicroelectronics LPS22HH [18] is 260-1260 hPa (26-126 kPa), in contrast to the 0.8–120 kPa Bounder range. The LPS22HH accuracy is 0.05 kPa, with a low-pressure sensor noise of 0.65 Pa. The digital output is specified as 24 bit, and its sensitivity as 4096 LSB/hPa.

It is known that height above the ellipsoid from GNSS constellations has relatively large errors, and we can use the barometer as a secondary estimate for height. We expect the Bounder barometer to perform much better at high elevation as it can go down to 0.8 kPa. Barometric pressure is transitory and depends strongly on the specific time and location. Since the Bounder provides independent measures of the height and pressure, we can construct an empirical function to compute height from pressure for the balloon height profile. Since pressure is expected to drop as the exponential of height, we performed a polynomial fit to the natural logarithm of scaled pressure. The method for the polynomial fit is provided in the redvox-pandas repository as the function `bounder_model_height_from_pressure`.

Figure 4 compares the Bounder and S10 barometer data, showing divergence above 20 km heights. We assume the Bounder barometer will be the most accurate of the two as its low-pressure specifications are better matched to the ~36 km height of this case study. Note the sample rate of the Bounder is ~1 Hz, whereas the sample rate of the S10 barometer is ~24 Hz.

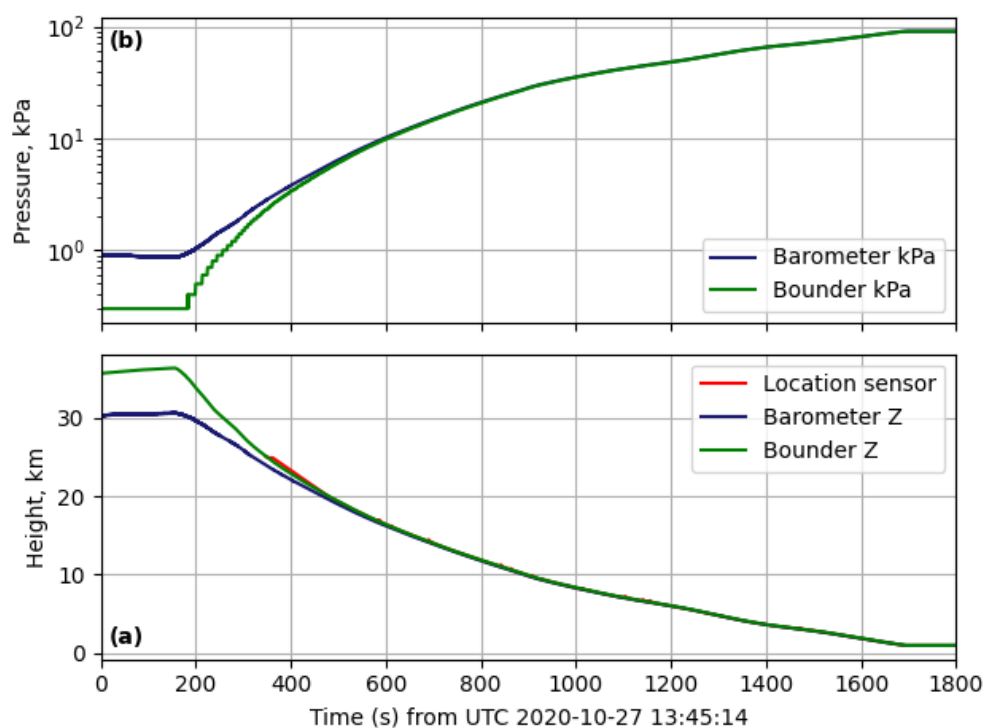


Figure 4. Comparison of barometer in Bounder and S10, and height above the ellipsoid from the Bounder, and the S10 inferred from the Barometer and Location sensor.

2.3.3. Accelerometer and Gyroscope

The Accelerometer and Gyroscope specifications obtained through the Android framework under RedVox API900 are listed in Tables 7 and 8.

Table 7. Accelerometer Sensor

Description	Field	Value
Sensor Name	station.accelerometer_sensor().name	LSM6DSO Accelerometer
Sample Rate Hz	station.accelerometer_sensor().sample_rate_hz	401.0575129
Sample Interval s	station.accelerometer_sensor().sample_interval_s	0.002493408
Interval Dev s	station.accelerometer_sensor().sample_interval_std_s	0.001007224

Table 8. Gyroscope Sensor

Description	Field	Value
Sensor Name	station.gyroscope_sensor().name	LSM6DSO Gyroscope
Sample Rate Hz	station.gyroscope_sensor().sample_rate_hz	401.057526
Sample Interval s	station.gyroscope_sensor().sample_interval_s	0.002493408
Interval Dev s	station.gyroscope_sensor().sample_interval_std_s	0.000992285

The documentation sheet for the ST Microelectronics LSM6DSO [19] 3D always-on, low-power accelerometer and gyroscope is thorough. This component has many possible configurations; the specific S10 configuration parameters are not saved under API 900, and a high level of detail is not available under the Android framework.

2.3.4. Magnetometer

The magnetometer specifications obtained through the Android framework under API900 are listed in Table 9.

Table 9. Magnetometer Sensor

Description	Field	Value
Sensor Name	station.magnetometer_sensor().name	AK09918 Magnetometer
Sample Rate Hz	station.magnetometer_sensor().sample_rate_hz	100.1370283
Sample Interval s	station.magnetometer_sensor().sample_interval_s	0.009986316
Interval Dev s	station.magnetometer_sensor().sample_interval_std_s	0.001235985

The specification sheet for the Asahi Kasei AK09918 3-axis Electronic Compass [20] provides a nominal sensitivity of 0.15 microTesla/LSB and states the digital output is 16-bit per axis.

2.3.5. Station State of Health Information

The state of Health (SOH) information supported by the API 900 framework is minimal, and consists of the station internal temperature and remaining battery percentage. This information is useful for maintaining station uptime, as sustained temperatures below 0 C and exceeding 40 C impact mobile device's batteries and battery charging capabilities. The device's battery status and temperature information are collected once per packet, which is 32.8 seconds in API 900 at 8000 Hz audio sample rate, corresponding to 2^{18} points per packet. Although useful, the coarse temporal granularity of the SOH information under API 900 is marginal for SWAP-C optimization.

API M has expanded SOH recording capabilities to include network type, network strength, data transmission rate, temperature, cell service state, battery remaining, battery current, available RAM, available disk, CPU utilization, power state, and WiFi wake lock, when available. Note not all hardware and operating systems make these sensors accessible. The API M apps permits collection of SOH data once per packet or once per second, where the packet length is also configurable.

2.4. Station Timing, Orientation, and Location

When, where, and how a recording station is deployed is captured by various sensor fields. In the simplest scenario, the station is stationary and connected to a stable communication network. For Skyfall, the station only stops moving after the payload hits the ground, rolls over, and is dragged by the parachute.

2.4.1. Timing

There are various timelines available to a smartphone. When first booted a smartphone internal clock does not know the time, and it would naturally go to the Unix epoch time zero of 1 January 1970 00:00 UTC. It will try to find time via GNSS, cell, or wifi. The operating system time (OS time) will use any and all available combinations to update its internal clock. OS time will jump back and forth as needed to keep up with the various clocks at its disposal. GNSS time will also jump about depending on which satellites are available. A third timeline, the machine time, is initialized when the unit is booted. Although the machine time is monotonic, it is only as accurate as its internal oscillator. Accurately estimating true time is beyond the scope of this work; our aim is to get an

estimate of timing errors for a given network configuration relative to a reference clock. In this case, the reference clock is at Amazon Web Services and it is only available when there is either cellular or wifi connectivity.

The application uses well-established tri-message exchange algorithms for synchronization and relies on three assumptions: that the message propagation delay is nearly symmetrical, errors of the timestamp itself have been mostly compensated, and the clocks' skew is negligible during the message exchange. The synchronization process starts when the reference server sends a message of its current timestamp to the device, the device then records the time of receipt and returns the message after a delay with its current timestamp and the server records the time of receipt. Using the time stamps we can find the average latency to calculate the offset between the clocks, the best-fit offset is selected by finding the best minimal statistically significant latency to compute the offset.

Timing correction is built into the RedVox SDK, and is only possible when communication is available to either a reference synchronization clock or GNSS satellites during data collection.

2.4.2. Station Orientation

The S10 coordinate frame follows the Android and iOS smartphone-centered cartesian xyz axis, with z positive away from the screen (Figure 5). A smartphone accelerometer laying screen up on a flat level surface has a constant value of -9.8 m/s^2 in the z axis. If the long horizontal axis (y) is pointing towards the North, the magnetometer x axis should be zero and the z axis will be the projection of the magnetic line on the vertical. The gyroscope will respond to rotation around the specified axis, positive counterclockwise (right hand rule), and shown by rotation arrows in Figure 5.

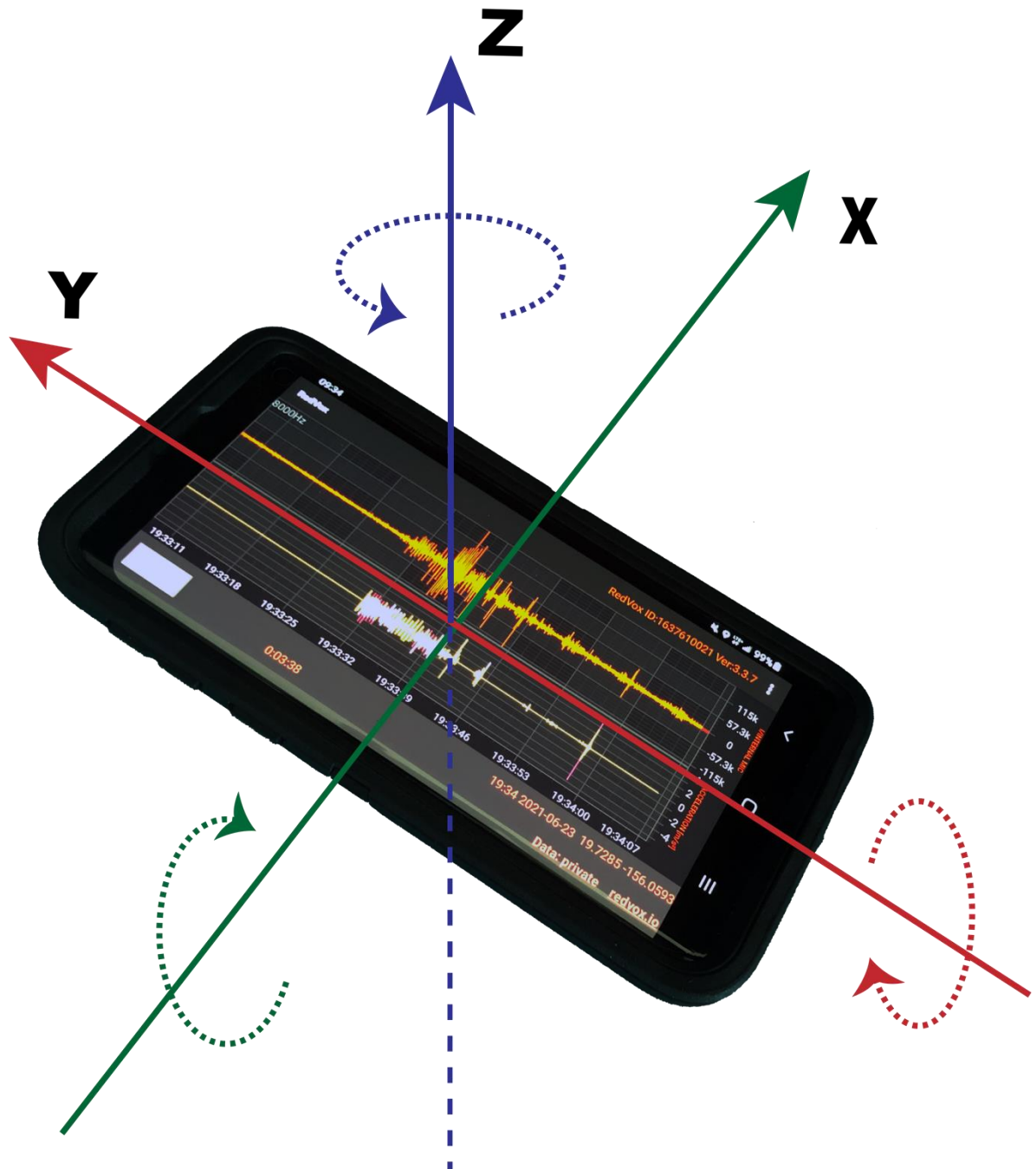


Figure 5. Reference frame for three component (3C) smartphone sensors.

2.4.3. Smartphone Location

As with timing, a smartphone will attempt to get its location via GNSS, cell, or wifi. Skyfall represents an extreme high-altitude collection event, and the location framework did not perform well above 20 km height (twice aircraft cruising altitudes) as there is a data gap. The RedVox API900 did not collect sufficient location information to disambiguate between cell, wifi, or GNSS location. This omission is corrected under API M.

Table 10. Smartphone Location Sensor

Description	Field	Value
Sensor Name	station.location_sensor().name	GNSS
Sample Rate Hz	station.location_sensor().sample_rate_hz	0.709595563
Sample Interval s	station.location_sensor().sample_interval_s	1.409253456
Interval Dev s	station.location_sensor().sample_interval_std_s	12.22592513

However, the location data that was obtained matched the boulder location (Figure 6) within the vertical scale of descent (km). As shown in Figure 7, synchronization via cell did not begin until the S10 dropped below 10 km. The spike just before 800 s probably corresponds to communications from a different cell tower. This suggests the height measurements above 8 km were from GNSS.

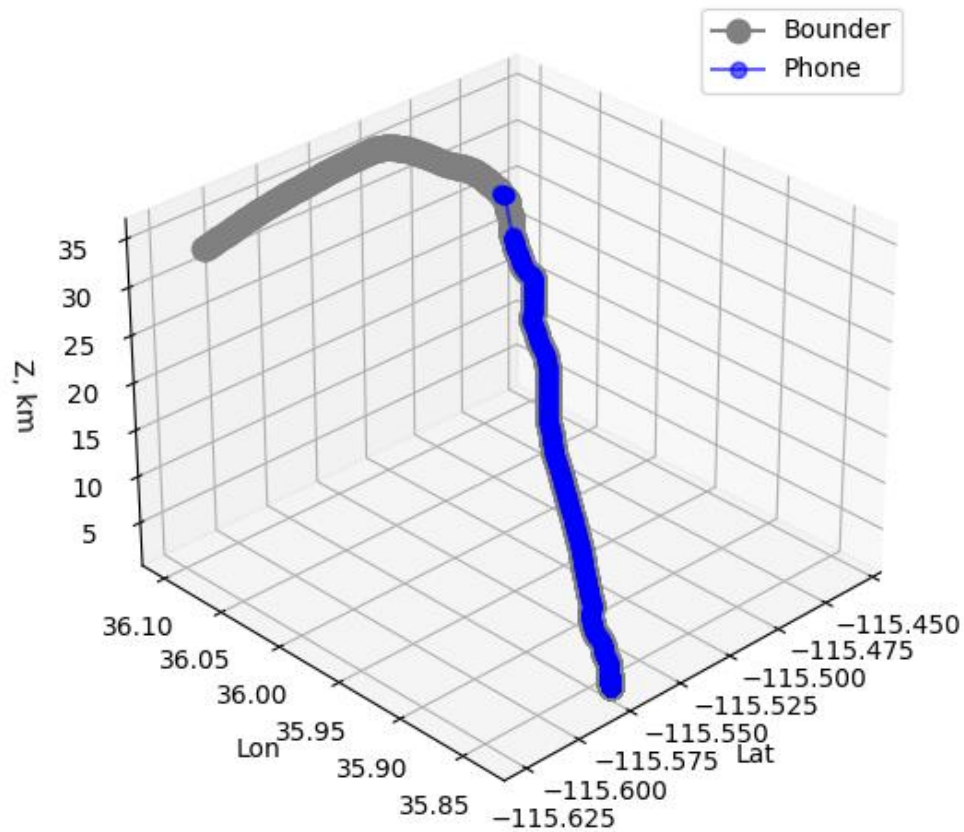


Figure 6. Comparison between Boulder and smartphone location.

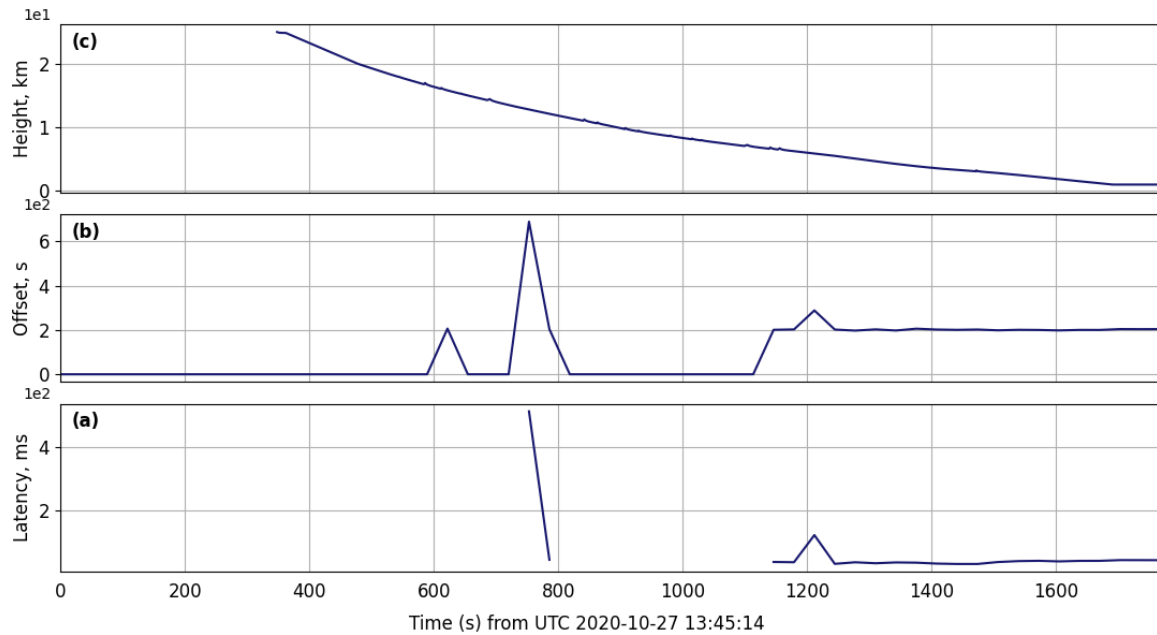


Figure 7. Timing synchronization framework showing (a) the estimated round-trip sync exchange latency in ms, (b) the station clock offset correction from the reference clock in seconds, and (c) location height above ground in km. There is a single latency point after 600 s that does not show in the line graph.

3. Results

Each sensor modality provides useful and complementary information on the descent chronology, as well as reveals the capabilities and limitations of the sensor system. This section seeks to reconstruct the Skyfall chronology from the available Bounder and smartphone data.

3.1.1. Bounder location and estimated speed

The Bounder platform provided the most complete record of the payload position, although it does not contain information about its orientation. The Bounder position is converted to cartesian East North Up (ENU) XYZ coordinates in Figure 8 to show its trajectory with time relative to the end of flight terminus. A scalar speed is computed from the derivative of the cartesian coordinates in Figure 8, and shown in Figure 9. The speed direction follows the trajectory. The balloon was moving briskly (~ 50 m/s) towards the Southeast in the upper stratosphere (above 25 km) when it began its descent, but swerved to the Southwest in the troposphere (below 10 km). The fastest descent was when it was released, when it hit a top speed of ~ 80 m/s. It slowed down as the parachute deployed in the thin, cold stratosphere, and then it approached the troposphere where it was struck by a shearing wind that reversed its Eastward journey. Surprisingly, it sped up again in the upper troposphere; whether this was due to a parachute malfunction or strong winds is unclear from the location record.

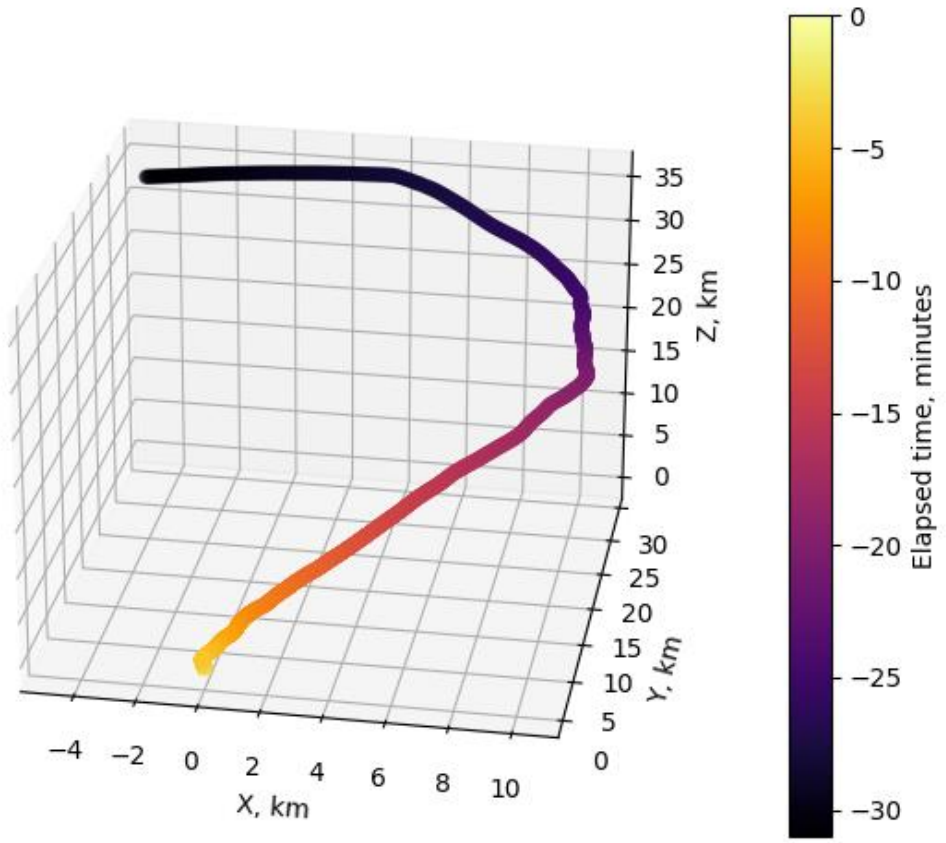


Figure 8. Boulder height chronology relative to the end of the record.

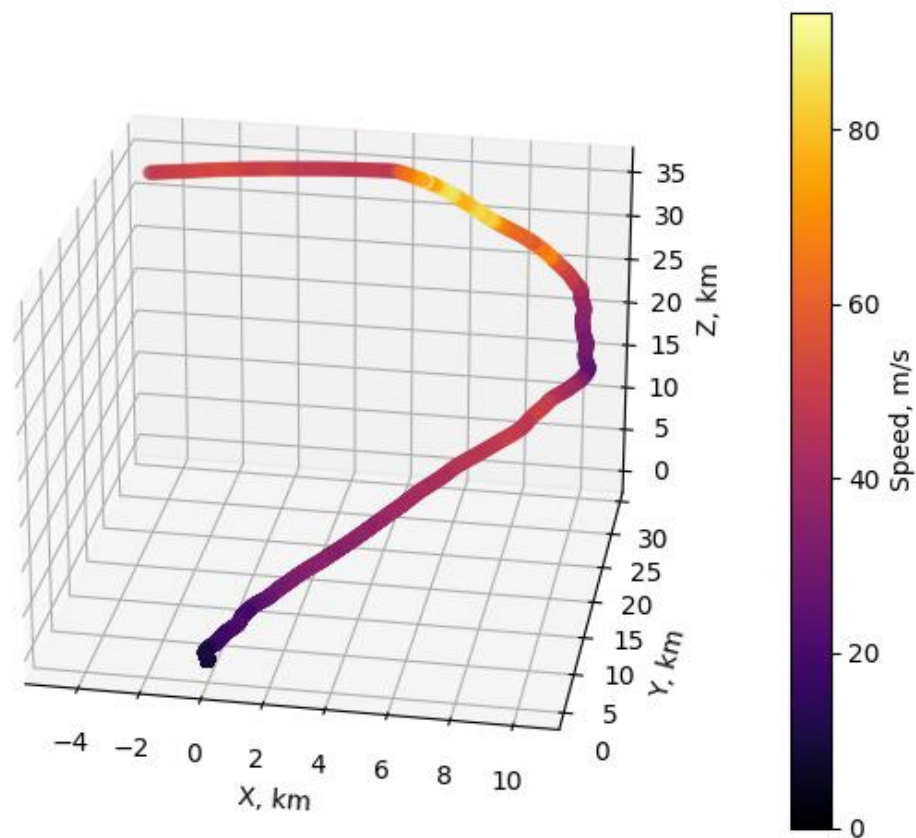


Figure 9. Bouncer speed estimated from position.

3.1.2. Smartphone location and estimated speed

The S10 smartphone location failed to provide location data above ~20 km (Figure 10). Once the payload was well on its descent, but only after its maximum descent speed, did the S10 begin to record a location. Although the location and speed values are comparable to the Bouncer, the S10 location data gap at height remains an unexpected surprise. As inferred from the synchronization data, cell position was only available below ~8 km. In summary, below 20 km and up to its terminus, the S10 location framework performed adequately (but not exceptionally) well, and was the first sensor to report its position upon landing. Both the Bouncer and the S10 show two regions of slow, near-vertical descent, likely where horizontal winds were low and the parachute performed as specified. The parachute reached its nominal 6 m/s descent rate in the lower troposphere before landfall, when it mattered most.

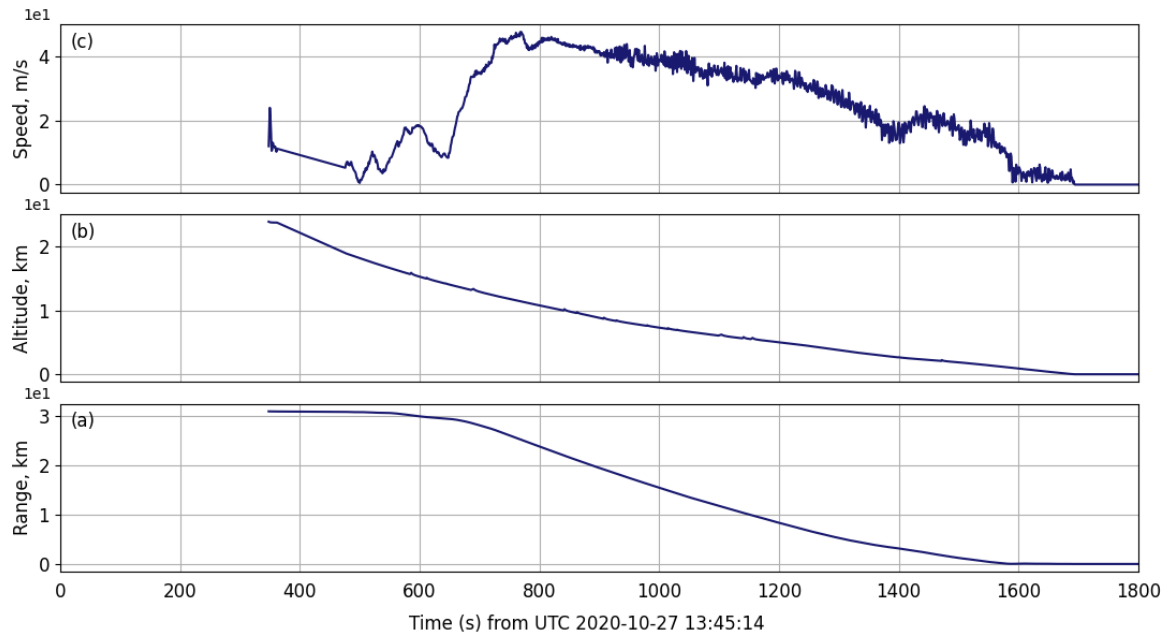


Figure 10. Range, altitude, and speed inferred from the phone location framework. It did not report during the fastest descent, but it performed adequately below 20 km. The descent speed was in excess of 10 m/s in the upper troposphere until it reached the lower troposphere where the atmosphere is most dense.

3.1.3. SOH Power and Temperature

The station power and temperature were coarsely sampled at intervals of ~ 30 s. Not surprisingly, the internal battery was discharging during the descent. The reported internal temperature of the station dipped below -8°C before it appears to rise again after the terminus. It is likely the station would have shut down and/or drained power rapidly had such low temperatures persisted. Additional SOH parameters at finer sample intervals will be collected under API M.

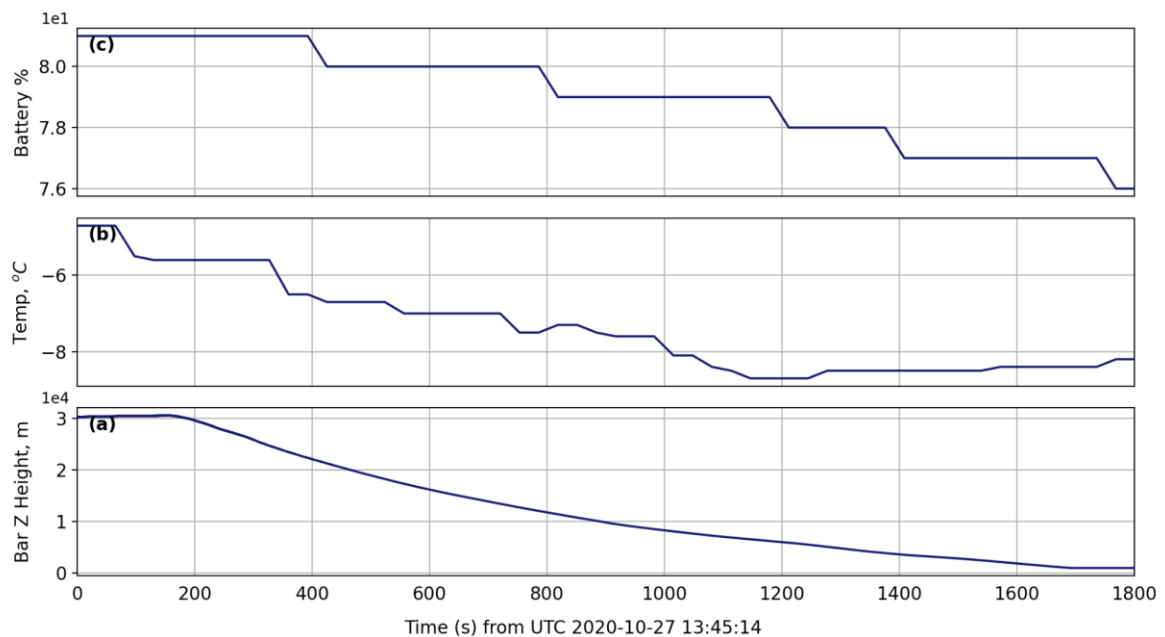


Figure 11. Power status during Skyfall descent showing (a) pressure during fall, (b) temperature, and (c) remaining battery percentage.

3.1.4. Acoustic pressure, barometric pressure, and vertical acceleration

The microphone, barometer, and vertical accelerometer sensors provide useful insight into Skyfall. These three channels are often complementary during ground-based measurements and are thus presented together. The audio channel, raw vertical acceleration, and height inferred from the barometer data are presented in Figure 12. There is not much audio signal during the release, but flow noise does increase during descent. The payload hits the tropopause (~10 km) halfway through the record (~900 s), and the ground impact is evident at ~1700 s. Figure 12 suggests that the S10 was laid down screen down, with gravity pointing up before release (+9.8 m/s). The release was a turbulent event with some tumbling, as suggested by the oscillations in the vertical acceleration. At the terminus, the payload enclosure flipped over, reversing the sign of gravity (-9.8 m/s). The microphone (mic) channel also clearly shows the impact.

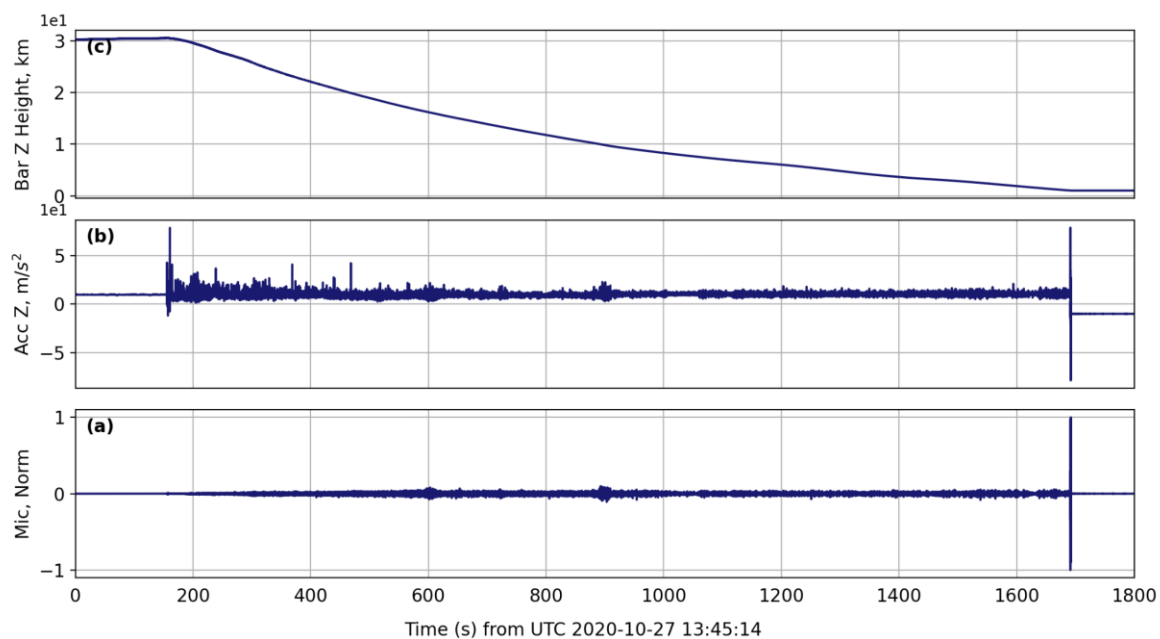


Figure 12. Sensor payloads for (a) audio, (b) z-component acceleration, and (c) height inferred from barometric pressure.

High-pass filtering the signal above 100 Hz (Figure 13) enhances the fine-scale variability in the barometer and vertical acceleration sensors, in particular for the barometric pressure. The sudden stop at the end (with a deceleration >6G) produced an overpressure of ~400 Pa in the barometer and, unsurprisingly, clipped the microphone.

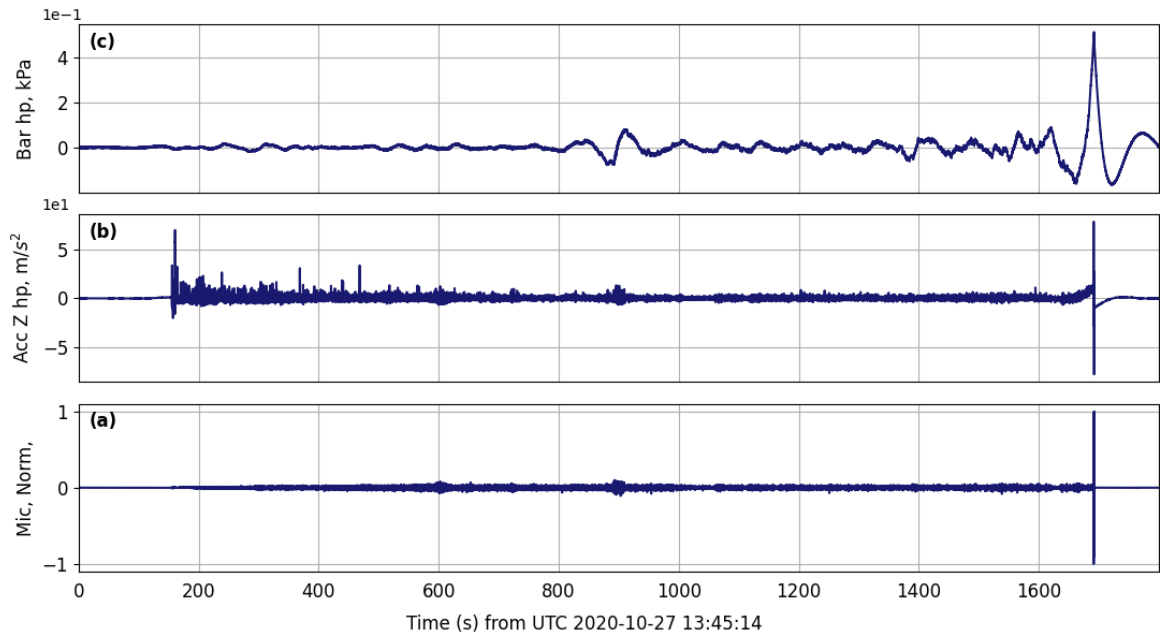


Figure 13. Sensor payloads for (a) audio, (b) high-pass filtered z-component of acceleration, and (c) high-pass filtered barometric pressure.

3.1.4. Three-component sensors: Accelerometer, Gyroscope, and Magnetometer

The three-component (3C) sensors provide insight into changes in the orientation of the payload. Accelerometers are included in almost all smartphones to detect when the device is picked up, and for gaming apps. Gyroscopes are often bundled in with accelerometers to correct for a smartphone's rotational orientation relative to gravity (e.g. screen orientation), and magnetometers are used for navigation. All the 3C channels are sampled unevenly, and show three clear stages of descent: the release of the payload with a freefall in the low-density stratosphere, the transition to the denser atmosphere in the tropopause at ~ 900 s, and the impact with the ground. The accelerometer suggests the phone was deployed screen down, and remained so through most of the turbulent descent. The horizontal (X-Y) channels show high accelerations during the stratospheric descent, and stabilized penetrating into the troposphere.

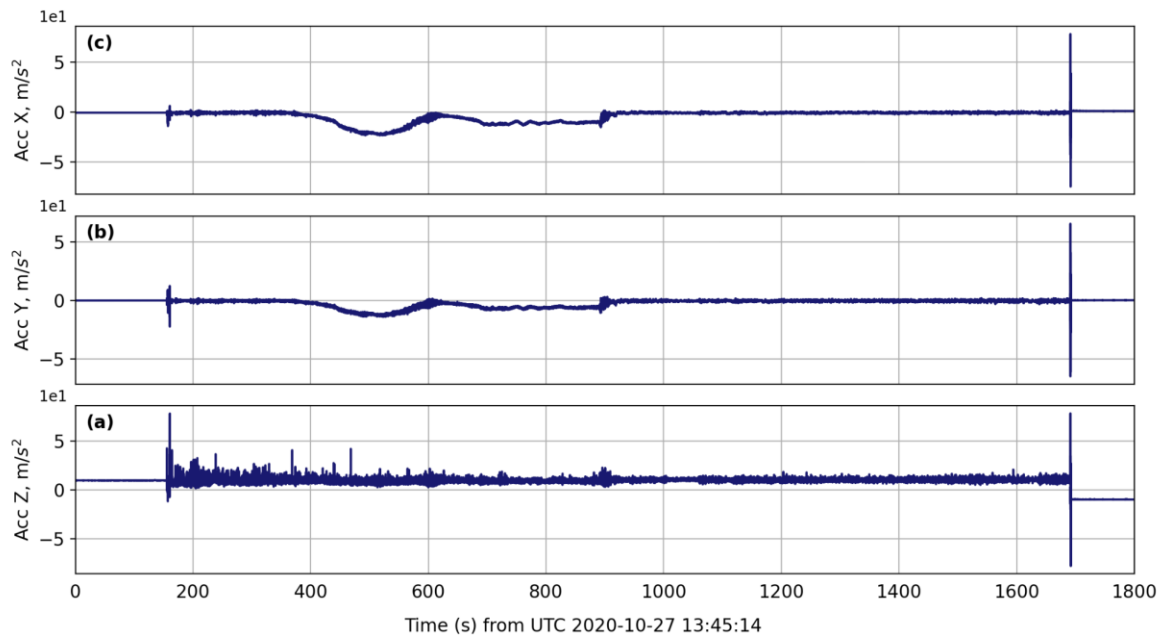


Figure 14. Acceleration channel payload for (a) z-direction component, (b) y-direction component, and (c) x-direction component.

All three gyroscope channels in Figure 15 indicate a stable payload while tethered to the balloon with the initiation of rapid rotation after release. The gyration about the horizontal X and Y axes (panels (c) and (b) in the figure, respectively) along the base of the payload box are dominated by fluctuations about 0 rad/s during the descent, while the Z channel (panel (a)) appears to show continuous and rapid rotation of the device about the Z axis from approximately 300 to 900 seconds into the descent through the stratosphere. The maximum rotation rate is 13.43 radians/second (2.14 rotations/s). After the 900 second mark, after entry into the troposphere, the readings drop and fluctuate about 0 rad/s. All channels spike at ground impact.

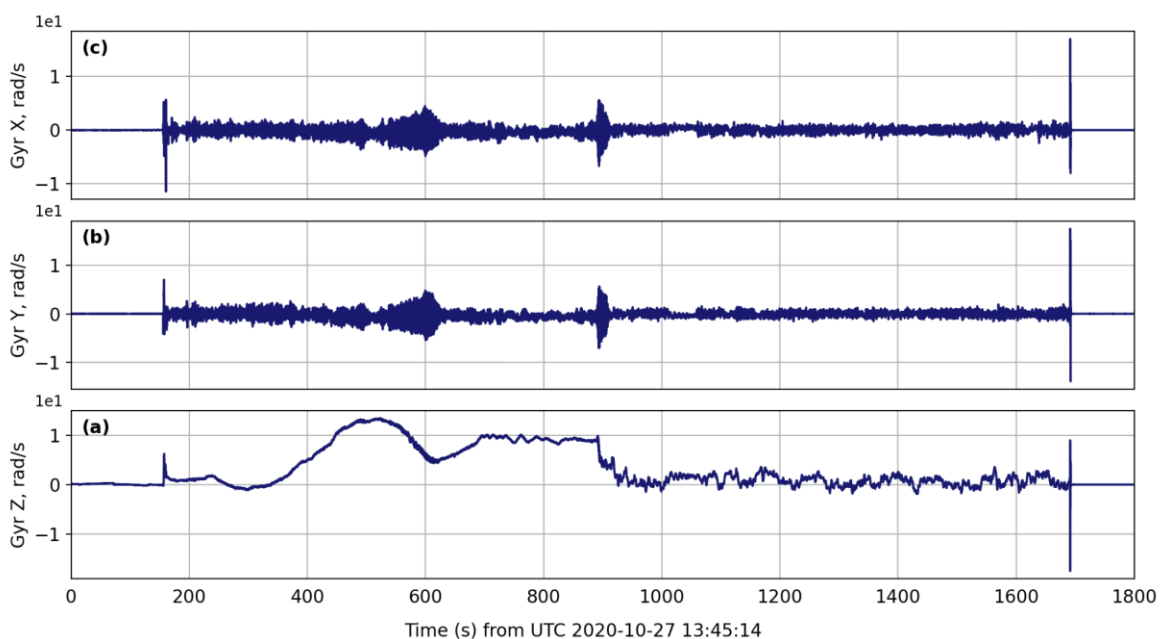


Figure 15. Gyroscope channel payload for (a) z-axis component, (b) y-axis component, and (c) x-axis component. The maximum rotation rate is 2.14 rotations/s (~ 2.14 Hz) about the z axis.

Data collected by the magnetometer along the three axes of the device are shown in Figure 16. A slow rotation about the z axis is evident while tethered to the balloon, while the magnetic line component along the z axis is stable. In the X and Y directions (shown in panels (b) and (c), respectively), readings oscillate about 0 μT during descent. For both the X and Y channels, the frequency is markedly higher from about 350 to 950 seconds into the descent. The amplitudes, however, are similar throughout the descent for both the X and Y channels. The data in the Z direction are shown in panel (a). Unlike those of the other channels, the readings in the Z direction do not oscillate about 0 μT , but instead remain near -5 μT after the initial moments of the descent, indicating that the compass direction of the Z axis remained relatively steady during the rapid descent, flipping only upon impact as inferred from the vertical accelerometer channel.

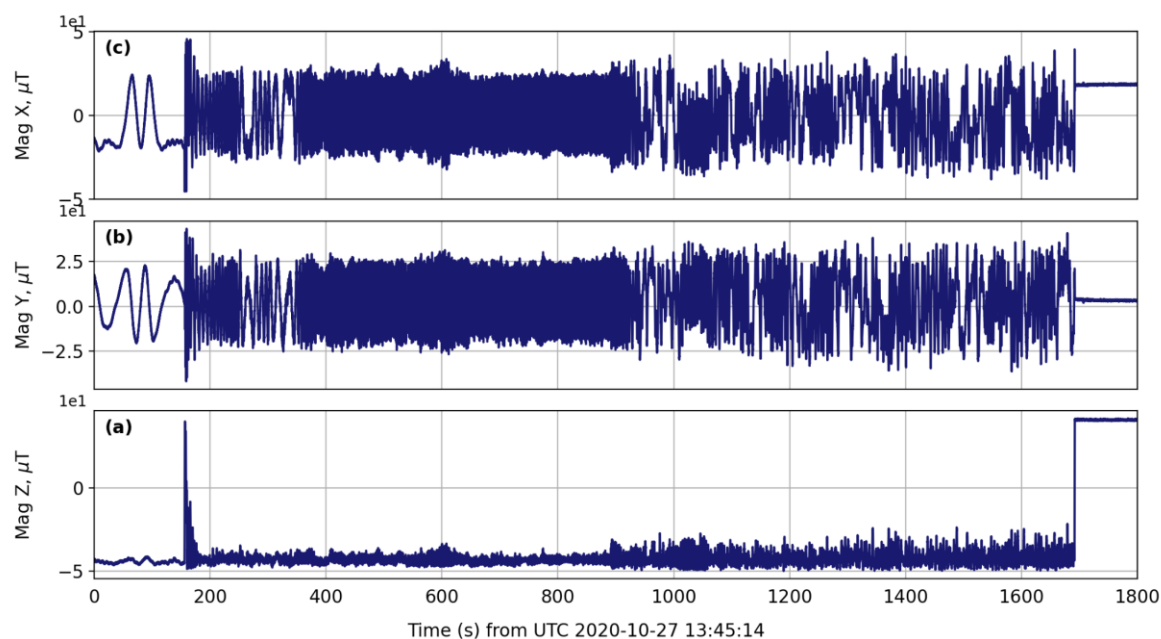


Figure 16. Magnetometer channel payload for (a) z-direction component, (b) y-direction component, and (c) x-direction component.

High-passed filtered channels are shown in Figure 17, with their corresponding estimated short-term Fourier transforms in Figure 18. The waveform plot amplitudes are normalized relative to the maximum values. The three main stages of the Skyfall are clear in all channels: initiation, transition to troposphere, ground impact. Throughout the flight and descent, the payload is in a flat spin along the vertical axis, with different rates of rotation at different stages; slow before descent, frantic (>10 rad/s) in the stratosphere, slowing down in the thermosphere. The tonal structure in the spectra in the rotation-sensitive channels (Figure 18) is a measure of the flat spin rotation frequency, and there is no evidence for tumbling. The payload flips over only after impact.

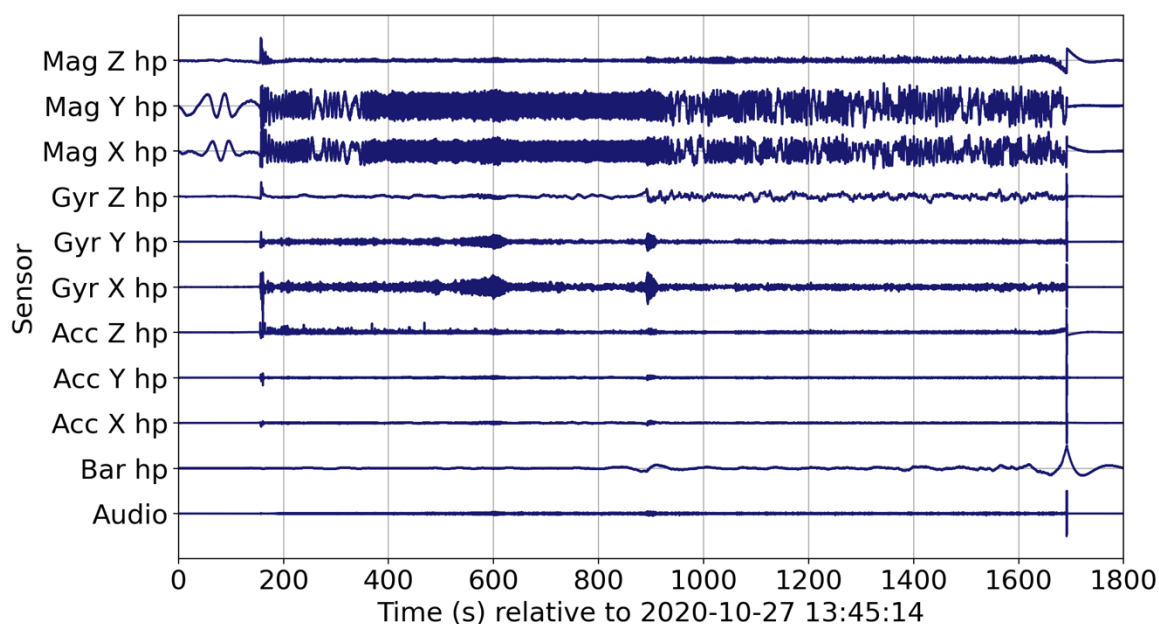


Figure 17. High pass filtered (hp) waveforms for sensors: audio, barometer (Bar), accelerometer (Acc), gyroscope (Gyr) and magnetometer (Mag). The vertical axes are normalized to the peak absolute magnitude of each channel.

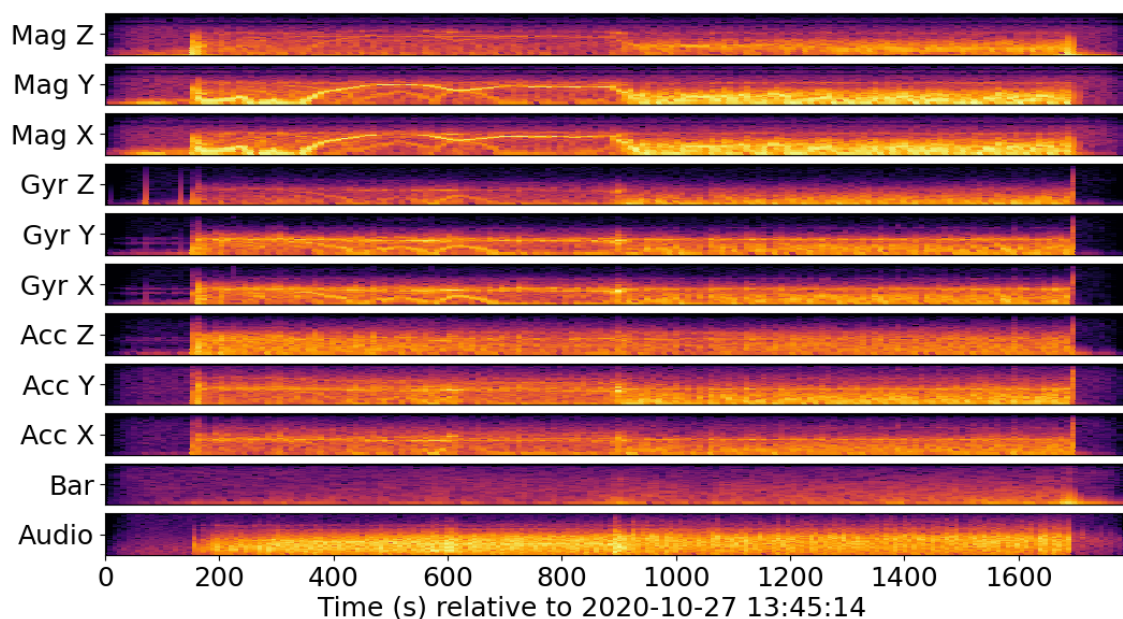


Figure 18. Short-term Fourier Transforms of high pass filtered (hp) waveforms for sensors: audio, barometer (Bar), accelerometer (Acc), gyroscope (Gyr) and magnetometer (Mag). The color scales to the maximum amplitude. The vertical axes represent logarithmic frequency in Hertz to the sensor Nyquist. The standardized minimum frequency scales with the record duration and the sample rate [21].

The gyroscope spectra reinforce the time-domain representation, as expected. More interestingly, the X and Y components of the magnetometer spectrograms confirm the ~ 2 Hz maximum revolution rate of the payload in the stratosphere. The magnetometer was sampled at ~ 100 Hz, with a Nyquist frequency at 50 Hz. The base-2 logarithm (bits)[21] of the spectral magnitude of the X component of the magnetometer is shown in Figure 19. As expected, the peak spectral

magnitude envelope matches the vertical component of the gyroscope in Figure 15, with a peak revolution rate of ~ 2 Hz.

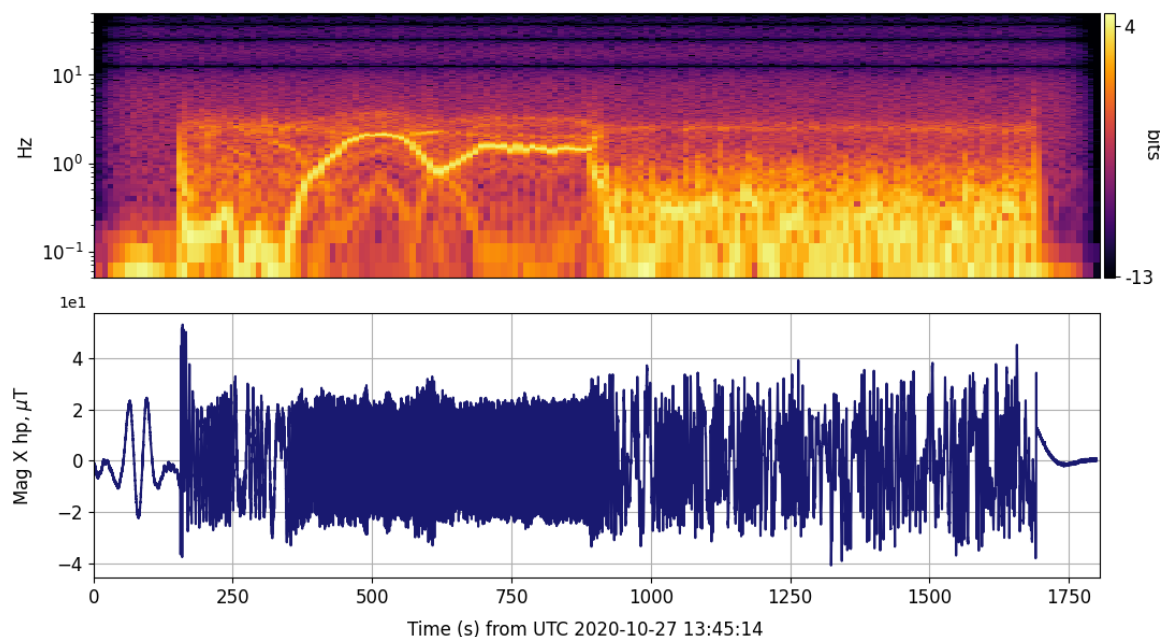


Figure 19. Short-term Fourier Transforms of high pass filtered (hp) waveforms for the X component of the magnetometer (Mag); the Y component is nearly identical.

Raw data and python code are provided to reconstruct the results in this paper, as well as produce additional results not presented herein. The reader is welcome to explore these openly-available data and software to search within the various intriguing spectral patterns within each channel.

4. Discussion and Conclusion

We described some of the internal smartphone sensor components and configurations that are accessible through the Android OS and the RedVox API for a Samsung Galaxy S10. The first-of-kind smartphone deployment in a high-altitude balloon and parachute to the ground provided useful and verifiable data [1]. This is the first scientific study of such an extreme phone data collection and drop test, and presents smartphones as viable sources of geophysical data.

The Bounder and S10 data study present a cohesive narrative. At the beginning of the record, the balloon is ascending through the stratosphere with the payload slowly spinning about its vertical axis. The Skyfall event begins with the dropping of the payload and substantial movement and rotation along all axes. The fastest descent occurred during the initial freefall. The first stage of the Skyfall event is the fall through the thin stratosphere, where the parachute has little to work with. The second stage corresponds to penetration into the troposphere and a reduction in rotational motion of the payload enclosure. The Skyfall terminates with impact on the ground, as shown by high amplitudes on all channels. The final minutes of the record show the payload enclosure flipped upside down and remains static and awaiting recovery.

There is an abundance of fine structure within the records and their spectra that can be explored by the interested researcher, as all data and software are openly available. Ongoing and future [5] research will use these frameworks and methods to study signals of interest on Earth and beyond.

Supplementary Materials: The following are available online at www.mdpi.com/xxx/s1, Figure S1: title, Table S1: title, Video S1: title. The raw data are openly available at <http://redvox.io/@/3f3f>, the RedVox SDK is at <https://pypi.org/project/redvox/>, and the Python software used to process the data and construct the figures is at <https://pypi.org/project/redvox-pandas/>.

Author Contributions: Conceptualization, M. Garces, D. Bowman, C. Zeiler; methodology, software, A. Christe, T. Yoshiyama, M. Colet; validation and analysis, B. Williams, M. Colet, S. Takazawa, S. Popenhagen, Y. Hatanaka, J. Tobin; resources, D. Bowman, C. Zeiler, K. McLin; data curation, T. Yoshiyama, M. Colet; writing—original draft preparation, M. Garces; writing—review and editing, all authors; supervision, M. Garces. All authors have read and agreed to the published version of the manuscript.

Funding: This paper was supported by the Department of Energy National Nuclear Security Administration under Award Numbers DE-NA0003920 (MTV) and DE-NA0003921 (ETI).

Disclaimer: This report was prepared as an account of work sponsored by agencies of the United States Government. Neither the United States Government nor any agency thereof, nor any of their employees, makes any warranty, express or implied, or assumes any legal liability or responsibility for the accuracy, completeness, or usefulness of any information, apparatus, product, or process disclosed, or represents that its use would not infringe privately owned rights. Reference herein to any specific commercial product, process, or service by trade name, trademark, manufacturer, or otherwise does not necessarily constitute or imply its endorsement, recommendation, or favoring by the United States Government or any agency thereof. The views and opinions of authors expressed herein do not necessarily state or reflect those of the United States Government or any agency thereof. The United States Government is authorized to reproduce and distribute reprints for Governmental purposes notwithstanding any copyright notation thereon.

Acknowledgments: The author is grateful for anonymous reviewers who helped improve the manuscript.

Conflicts of Interest: The author declares no conflict of interest. The funders had no role in the design of the study; in the collection, analyses, or interpretation of data; in the writing of the manuscript, or in the decision to publish the results.

References

1. Popenhagen, S., Garcés, M. A., Bowman, D., Zeiler C. Analysis of explosion data collected on an airborne platform, NNSA University Program Review (UPR), 8-10 September 2021, Atlanta, GA.
2. RedVox for Android on the Google Play Store. Available online: <https://play.google.com/store/apps/details?id=io.redvox.InfraSoundRecorder&hl=en>
3. RedVox for iOS and M1 chip on Apple App store. Available online: <https://apps.apple.com/sz/app/redvox-recorder/id969566810>
4. Balloon Ascent Technologies HAB Bouncer Balloon Cut-Down Device. Available online: https://loonatec.com/blog/wp-content/uploads/2020/09/HAB_Bouncer_User_Guide_rev5.pdf
5. Takazawa, S., M. A. Garcés, L. O. Giraldo, J. Hix, S. Watson, D. Chichester, C. Zeiler (2021). Explosion Data Fusion of Acoustic, Barometric, and Accelerometric Data Collected on Smartphones, University Program Review (UPR), 8-10 September 2021, Atlanta, GA.
6. RedVox Application Programming Interface (API). Available online: <https://github.com/RedVoxInc/redvox-api-1000>
7. RedVox Software Developer Kit (SDK). <https://github.com/RedVoxInc/redvox-python-sdk>
8. RedVox-Pandas Framework. Available online: <https://github.com/RedVoxInc/redpandas>,
9. McKinney W, others. Data structures for statistical computing in python. In: Proceedings of the 9th Python in Science Conference. 2010. p. 51–6. Available Online: <https://pypi.org/project/pandas/>
10. Raw Skyfall data available from the collection of event reports at RedVox.io Analysis/Featured Events. Available online at: <http://redvox.io/@/3f3f>
11. Totex Corporation Meteorological Balloon. Available online: https://totex.info/hinmoku_kikyuu_e.html
12. Rocketman Parachutes. Available online: <https://the-rocketman.com/>
13. High Altitude Science StratoTrack APRS. Available online: <https://www.highaltitudescience.com/products/stratotrack-aprs-transmitter>
14. Globalstar SPOT Trace. Available online: <https://www.globalstar.com/en-us/products/spot-for-business/spot-trace>
15. Samsung Galaxy S10 specifications, <https://www.samsung.com/global/galaxy/galaxy-s10/specs/>
16. Asmar, K., Garcés, M. A., Williams B. A method for estimating the amplitude response of smartphone built-in microphone sensors below 4 kHz. *J. Acoust. Soc. Am.* 2019, 146 (1).

17. Asmar, K., Hart, D., Garcés, M. A., Williams, B. Digital acoustic sensor performance across the infrasound range in simulated field conditions. *J. Acoust. Soc. Am.*, 2018, 144 (5), <https://asa.scitation.org/doi/10.1121/1.5078591>
18. ST Microelectronics LPS22HH Barometer specifications, <https://www.st.com/resource/en/datasheet/lps22hh.pdf>
19. ST Microelectronics LSM6DSO Accelerometer and Gyroscope specifications, <https://www.st.com/resource/en/datasheet/lsm6dso.pdf>
20. Asahi Kasei Microdevices (AKM) AK09918 3-axis Electronic Compass specifications, <https://www.akm.com/content/dam/documents/products/electronic-compass/ak09918c/ak09918c-en-datasheet.pdf>
21. Garcés, M. A. Quantized constant-Q Gabor atoms for sparse binary representations of cyber-physical signatures, *Entropy*, 2020, 22, 936; doi:10.3390/e22090936